Endoglin and the immune system: immunomodulation and therapeutic opportunities for cancer

Schoonderwoerd, M.J.A.

4

Fibroblast-specific endoglin knock out changes the colonic immune infiltrate and increases formation of colitis associated intestinal adenomas

MANUSCRIPT IN PREPARATION

Mark J.A. Schoonderwoerd[1], Madelon Paauwe[1], Lars Ottevanger[1], Leonie Plug[1], Amelia Bassuki[1], Eveline S.M. de Jonge-Muller[1], Stef Janson, James C.H. Hardwick[1], Marieke F. Fransen[2], Lukas J.A.C. Hawinkels[1]

[1]Dept. of Gastroenterology-Hepatology, [2]Immunohematology and Blood Transfusion, Leiden University Medical Center, Leiden, The Netherlands

ABSTRACT

In addition to high endoglin expression on endothelial cells, endoglin expression has been reported on Cancer Associated Fibroblasts (CAFs) in solid tumors, including colorectal cancer (CRC). Although data indicate an important role in later stages of tumor development, the role of endoglin-expressing fibroblasts in early cancer development and its interaction with the immune system has hardly been investigated. Therefore, in this study we have generated a tamoxifen-inducible fibroblast-specific (col1a1 and col1a2) endoglin knock out mouse ($ENG^{Fib-/-}$). Tumor formation was studied using the azoxymethane/dextran sodium sulphate (DSS) model for colitis-associated cancer. Interestingly, a significant increase in the number of adenomas was observed in $ENG^{Fib-/-}$ mice compared with control mice. Analysis of infiltrating immune cells revealed that deletion of endoglin in fibroblasts resulted in enhanced recruitment of macrophages and neutrophils to AOM/DSS-induced adenomas. However, these neutrophils did not cause the increased tumorigenesis observed in the $ENG^{Fib-/-}$mice. To investigate the tumor initiation stage, a short DSS was performed, revealing in contrast to late stages, a decrease in the number of myeloid cells in both the colon as well as the blood of these mice. These data suggest a delayed immune response, which was reflected in the severe weight loss of the $ENG^{Fib-/-}$ mice. Together, these data suggest that endoglin expression on fibroblasts plays a role in the initiation of colitis induced CRC, potentially by altered or delayed inflammatory responses.

INTRODUCTION

Paracrine interactions between malignant epithelial cells and their tumor microenvironment (TME) play a crucial role in cancer progression [1, 2]. The TME of solid tumors, such as Colorectal Cancer (CRC), is composed of non-malignant cells, including tumor infiltrating inflammatory cells, endothelial cells forming the tumor vasculature system and cancer-associated fibroblasts (CAFs) [3]. CAFs compose the major part of the tumor stroma. CAFs are a diverse group of fibroblasts expressing vimentin, fibroblast activating protein (FAP) and α-smooth muscle Actin (αSMA) [4]. CAFs in solid tumors interact with other cells via several cytokines and direct cell-cell contact (reviewed in [5]). Members of the Transforming growth factor β (TGF-β) superfamily seem to play a central role in the generation of CAFs [6-8]. TGF-β is an extensively studied family of cytokines, both important in tissue homeostasis and cancer. Signaling is regulated via the expression of a distinct set of receptors and co-receptors. One of the TGF-β coreceptors is endoglin, which can interact with TGF-β and Bone Morphogenetic Protein 9 (BMP9) and regulate angiogenesis [9-13]. TGF-β can interact with endoglin and activate the ALK5-SMAD2,3 pathway, which causes blood vessel maturation. BMP9 can signal through the endoglin- ALK1-SMAD1/5/8 pathway, which causes migration and proliferation of endothelial cells [14-17]. In addition to very high endoglin expression on angiogenic endothelial cells, we and others have observed endoglin expression on cancer associated fibroblasts (CAFs) in both Prostate [18] and CRC [19]. In CRC, endoglin on CAFs seems to play a role in the development of CRC derived liver metastasis in experimental models. Although the role of endoglin on fibroblasts has been studied using endoglin heterozygous mice and targeted antibodies, these results poorly reflect the specific role of endoglin on fibroblasts.

Therefore, in this project, we aim to investigate the role of endoglin on fibroblasts during CRC initiation using the azoxymethane/dextran sodium sulphate (AOM/DSS) model [20]. This most commonly used model for colitis associated cancer generates tumors that resemble (early stage) human CRC [21]. To investigate the endoglin specific role on fibroblasts in tumorigenesis we generated a tamoxifen-inducible fibroblast-specific (col1a1 and col1a2) endoglin knock out mouse ($ENG^{Fib-/-}$). Tumor initiation and the role of infiltrating immune cells was further investigated in these KO mice.

MATERIALS AND METHODS

Cell culture, preparation of CM and signaling assays

Mouse fibroblasts and the mouse CRC cell line MC38 [22] were cultured in DMEM/F12, supplemented with 10% fetal calf serum (FCS), 10 mM HEPES, 50 µg/mL

gentamycin, 100 IU/mL penicillin and 100 µg/mL streptomycin (all ThermoFisher, Waltham, MA, USA). The mouse CRC cell line CT26 [23] was maintained in RPMI 1640, supplemented with 10% FCS, 100 IU/mL penicillin and 100 µg/mL streptomycin (all ThermoFisher). Murine embryonic fibroblasts (MEFs) were obtained from E12.5 embryos as described before [24], from an endoglin flox/flox mouse strain in which exons 5 and 6 are flanked by LoxP sites [25]. MEFs and the mouse myoblast cell line C2C12 were maintained in DMEM, supplemented with 10% fetal calf serum (FCS), 100 IU/mL penicillin and 100 µg/mL streptomycin (all ThermoScientific).
Constructs expressing Cre recombinase (pLV.mPGK.iCRE.IRES.PuroR, kindly provided by Dr. M. Goncalves, Dept.of Cell and Chemical Biology, Leiden University Medical Center) or empty vector control were delivered using lentiviral transduction using polybrene (4 µg/mL, Hexadimethrine bromide, Sigma Aldrich) to 80% confluent MEFs and after 48 hours, transduced cells were selected by 1.5 µg/mL puromycin (Sigma Aldrich).
Conditioned medium (CM) from MEFs was prepared by serum starving subconfluent cells for four days. CM used for proliferation assays was two-fold diluted with culture medium, containing 5% FCS.

MTS proliferation assay

5000 CT26 or MC38 cells were seeded in 96-well plates in triplicate. After 16 hours, the medium was replaced with 100 µL CM, from either control or endoglin knock out MEFs or with non-conditioned medium. At indicated time points 20 µL MTS substrate (Promega, Madison, WI, USA) was added to each well and absorbance was measured at 490 nm using a VersaMax plate reader (Molecular Devices, Sunnyvale, CA, USA).

Mice

The Dutch animal ethics committee approved all animal experiments. Collagen1α1-Cre/ERT2 and Collagen1α2-CRE/ERT,-ALPP mice were purchased from Jackson Laboratory (strain B6.Cg-Tg(Col1a1-cre/ERT2)1Crm and Tg(Col1a2-cre/ERT,-ALPP)7Cpd, Jackson laboratory Bar Harbor, ME, USA). ENG*fl/fl* mice in which exons 5 and 6 of the endoglin gene are flanked by LoxP sites were generated by Allinson et al. [25]. Before tamoxifen induction, mice were divided into two groups, based on sex and body weight. Cre-mediated recombination was induced at eight weeks of age by oral administration of 50 uL tamoxifen (100 µg/mL, Sigma-Aldrich, Zwijndrecht, The Netherlands) dissolved in sunflower oil, on three consecutive days. Control mice had the same genotype but were treated with sunflower oil only. Collagen1α1-CreERT2.ENG*fl/fl* or Collagen1α2-Cre/ERT,-ALPP.ENG*fl/fl* and ENG*fl/fl* mice were used for control experiments as described. Mice were genotyped by PCR for the presence of the Cre recombinase and endoglin LoxP gene as described before [19].

AOM/DSS model

Two days after tamoxifen induction male and female mice received one intraperitoneal (i.p.) injection with 10 mg/mL azoxymethane (AOM; Sigma-Aldrich, Zwijndrecht, The Netherlands) dissolved in saline. Two days later, the first 7-day cycle with 1.5% dextran sodium sulphate (DSS; MP Biomedicals, Santa Ana, CA, USA) dissolved in drinking water, supplemented with artificial sweetener (Natrena, Utrecht, the Netherlands), was started. After seven days, drinking water was changed to normal conditions for 14 days. This three-week cycle was repeated twice more during the experiment. During DSS cycles, mice weight and overall health were monitored daily, while during the "off" period animals were weighted and checked every other day. Two weeks after the third DSS cycle, mice were sacrificed, and blood and tissue samples were collected. Colons were partially snap-frozen in liquid nitrogen for RNA analysis and partially fixed in 4% formaldehyde and photographed by using a NIKON D750 camera equipped with a TAMRON 24-70mm f2.8 lens. Lesion volume was measured in photographed colons by ImageJ (National Institute of Health), and tumor volume was calculated (tumor volume = (width^2 × length)/2). For the short DSS induced colitis mice were sacrificed after the first cycle of DSS, blood and tissue samples were collected and possessed for histology and flow cytometry analysis.

Neutrophil (Ly6G) depletion

Ly6G depleting antibody was given either on the day of the start the first DSS cycle or the second DSS cycle followed by a twice weekly i.p. injection of 0.2mg antibody 1A8 or IgG control dissolved in PBS (BioxCell, West Lebanon, USA). Blood was monitored weekly during the time of depletion. Depletion was stopped once the neutrophils (GR-1+ Cells) repopulated the blood of the mice (after +/-20 days of depletion).

RT-qPCR

Tissue samples were disrupted using a TissueLyser (Qiagen, Hilden, Germany) and RNA was isolated using Nucleospin RNA kit (Bioké, Leiden, The Netherlands), according to manufacturers' instructions. For *in vitro* experiments, MEFs were grown to confluency, harvested and RNA was isolated according to manufacturers' instructions. RNA concentration and purity were determined using NanoDrop 3300 (Thermo Scientific, Breda, The Netherlands). Complementary DNA synthesis was performed using 1 µg RNA using RevertAid First Strand cDNA synthesis kit, according to manufacturers' instructions (ThermoScientific). Quantitative PCR analyses were performed as described before [19], using primers as described in supplementary table 1 (Invitrogen). All values were normalized by *GAPDH* expression.

Table 1. Assessment of inflammation by means of clinical and macroscopic score.

Score	Diarrhea score	Visible fecal blood	Inflammatory Score
0	Normal Pallets	Normal	Normal
1	Slightly loose feces	Slightly bloody	Slight inflammation
2	Loos feces	Bloody	Moderate inflammation and or edema
3	Watery diarrhea	Blood in the whole colon	Heavy inflammation and or ulcerations and or edema

Flow cytometry

Tumor material was minced with scalpels and digested with Liberase (Roche, Basel, Switzerland) (Sigma-Aldrich, Zwijndrecht, NL) 375 µg/ml DMEM/F12 containing 10% FCS for 30 minutes at 37°C. To obtain single cells, the suspension was filtered through Falcon™ Cell Strainers 70 µm pore size (Fisher Scientific, Landsmeer, NL, 352350) and both tumor as blood was stained with antibodies against CD45, CD11b (both eBioscience, Vienna, Austria), F4/80, Ly6C GR-1 and Ly6G (all BioLegend, San Diego, CA, USA). FACS analysis was performed on the LSR II system (Becton Dickinson, Breda, The Netherlands). Data were analyzed using FlowJo data analysis software (FlowJo, Ashland, OR, USA).

Tissue analysis

Immunohistochemical stainings were performed as described previously [26], using primary antibodies against vimentin, cleaved caspase 3 (both Cell Signaling Technologies, Danvers, MA, USA), αSMA (Progen, Heidelberg, Germany), Ki67 (Millipore, Amsterdam, The Netherlands), Ly6G (BioLegend), F4/80 (eBioscience) and endoglin (R&D systems, Abington, UK). For quantification of total collagen, tumor sections were stained with Sirius red (Klinipath, Duiven, The Netherlands). In short, paraffin sections were deparaffinized, stained with 0.1% Sirius red in picric acid, washed in 0.01M HCl and subsequently dehydrated and mounted in entellan. Three to five representative pictures per mouse were taken with an Olympus BX51TF microscope (Olympus Life Science Solutions, Zoeterwoude, The Netherlands) and staining was quantified using ImageJ software (National Institutes of Health). Quantification of macrophage infiltration was scored based on F4/80 staining. Score 1; ≤5% stroma positive, score 2; 5-25% stroma positive, score 3; 25-50% stroma positive, score 4; ≥50% stroma positive.

Macroscopic disease score

Macroscopic disease score (Table 1) was calculated by scores reflecting degree of diarrhea, visible fecal blood, and inflammatory score on the day of termination. The scores are characterized on a scale of 0-3 including half points. An experienced

technician conducted the score, the inflammatory score was judged by degree of inflammation and presence of ulcerations and or edema in the tissue. The total score was calculated by adding up the three individual scores and illustrated in the graph.

Statistical analysis

Data indicate mean ± SD, as indicated in figure legends. Differences between groups were calculated using Students' *t*-test, Mann-Whitney or ANOVA analysis when appropriate. P-values ≤0.05 were considered statistically significant.

RESULTS

Fibroblast-specific endoglin knock out enhances AOM/DSS-induced adenoma formation

To assess the effect of fibroblast-specific endoglin deletion in tumorigenesis, collagen1α1-Cre-ERT2 mice were crossbred with ENG*fl/fl* mice, generating collagen1α1-CreERT2.ENG*fl/fl* mice. Cre-mediated recombination was induced in 8-week-old animals by oral administration of tamoxifen, generating ENG$^{Fib-/-}$ mice. Animals were exposed to the AOM/DSS protocol, as described in figure 1A. During the first DSS administration mice from the ENG$^{Fib-/-}$ lost significantly more weight compared to the control mice suggesting enhanced colonic inflammation Figure 1 B. In the ENG$^{Fib-/-}$ group rectal blood loss, rectal prolapse and substantial weight loss, were more often observed, reflecting the more severe phenotype.

At the end of the experiment, the number of lesions in the colorectum was quantified. The occurrence of colonic lesions was significantly increased in the ENG$^{Fib-/-}$ group compared with control mice (Fig. 1C and D). Although the number of lesions differed significantly, the average lesion size was similar in both groups (Fig. 1E). Lesions were analyzed by H&E staining and adenomas with high-grade dysplasia were found in both groups (Fig. 1F). In addition, the number of adenomas was not dependent on the sex of the mice (Suppl. Fig. S1B). To exclude the possibility that endoglin deletion in fibroblasts results in spontaneous neoplastic growth, mice were induced with tamoxifen to obtain ENG$^{Fib-/-}$. Animals were kept for 13 weeks, identical to the experiment's time course, and did not receive AOM or DSS. At the end of the experiment, adenoma formation in the colorectum was assessed. In ENG$^{Fib-/-}$, no lesions in the colorectum were observed (Suppl. Fig. S1C). Additional histological analysis did not reveal any morphological changes in the colorectum. This suggests that fibroblast-specific endoglin knock out does not result in spontaneous neoplastic growth during our experiments.

Additionally, to assess the effect of tamoxifen administration on tumor induction, ENG*fl/fl* mice without the Cre recombinase, as a negative control, received oral

tamoxifen and were subsequently exposed to the AOM/DSS regimen as described in figure 1A. After 13 weeks, the number of adenomas in the colorectum of tamoxifen-induced ENG*fl/fl* mice was similar to non-induced Collagen1α1-CreERT2. ENG*fl/fl* mice treated with AOM and DSS (Suppl. Fig. S1C). This suggests that tamoxifen administration does not affect AOM/DSS-induced adenomas formation.

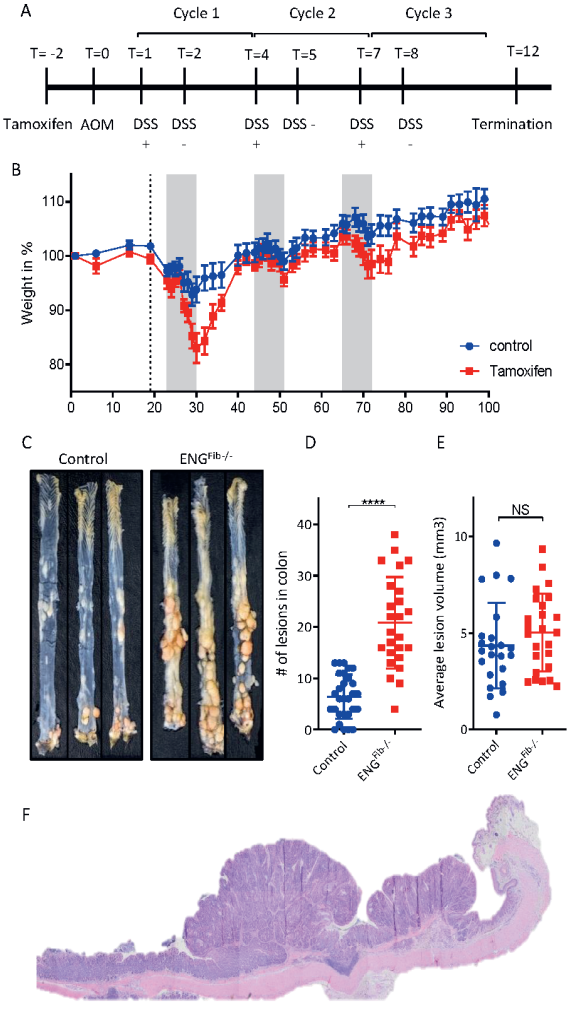

Figure 1. Fibroblast-specific endoglin knock out enhances AOM/DSS-induced neoplastic growth.
A. Experimental set-up. At 8 weeks of age, mice were induced with tamoxifen. After two weeks, AOM was injected, followed by three 21-day DSS cycles. Two weeks after the last DSS cycle, experiments were terminated. **B**. Representative pictures of colons obtained from control and fibroblast-specific endoglin knock out (ENGFibfl/fl) mice. **C**. Neoplastic growth was highly increased in ENGFibfl/fl mice, although size of the lesions was not different between the groups (**D**). Representative histological picture of a lesion qualified as high grate dysplasia by an independent pathologist. Graphs represent mean of 29-25 mice/group from two independent experiments. ****P≤0.0001.

These data imply that loss of endoglin on fibroblasts enhances colonic adenoma formation in chemically induced inflammation-driven colorectal cancer model.

Fibroblast-specific endoglin knock out does not affect epithelial proliferation

Since fibroblasts play an important role in intestinal homeostasis, we analyzed adenomas from control and ENG$^{Fib-/-}$ mice to assess changes. First, we determined the number of proliferating cells in AOM/DSS-induced adenomas using Ki67 as a marker for proliferating cells upon quantification, similar numbers of proliferating cells were observed in both groups (Fig. 2A). Next, we stained for the apoptotic marker cleaved caspase 3 to assess the number of apoptotic cells in the adenomas, apoptotic rates were similar in both control and ENG$^{Fib-/-}$ mice (Fig. 2B).
To confirm our *in vivo* observations the effects of endoglin deletion in fibroblasts on epithelial cell proliferation was assessed. Since knockdown of endoglin in primary fibroblasts results in a lethal phenotype *in vitro [19]*, murine embryonic fibroblasts (MEFs) from ENG*fl/fl* mice were used. Cre was introduced in these cells using lentiviral transduction, resulting in genetic deletion of endoglin (Fig. 2C). Conditioned medium (CM) from empty vector and endoglin knock out MEFs was prepared to assess paracrine signaling to mouse epithelial cells. Mouse CRC cells CT26 and MC38 were stimulated with CM from either empty vector control or endoglin knock out MEFs and proliferation was measured. Over the course of three days using an MTS assay, proliferation rates between non-stimulated cells, control CM or endoglin knock out CM stimulated cells were similar in both CT26 (Fig. 2D) and MC38 cells (Fig. 2E). This suggests that endoglin expression on fibroblasts does not directly affect epithelial tumor cell proliferation in a paracrine manner, confirming our *in vivo* findings.

Fibroblast-specific endoglin knock out increases stromal content

Since CRC tumors are generally characterized by an abundant stromal compartment, the effect of fibroblast-specific endoglin deletion on the adenomas' total stroma was assessed by staining for the mesenchymal marker vimentin. Adenomas from ENG$^{Fib-/-}$ mice showed a significant increase in vimentin-positive cells when compared with control mice (Fig. 3C). To assess the number of activated fibroblasts αSMA staining was used. As observed for vimentin, the percentage of αSMA-positive content was increased in ENG$^{Fib-/-}$ adenomass compared with the control (Fig. 3D). Although more αSMA-positive fibroblasts were observed in ENG$^{Fib-/-}$ adenomas, total collagen production determined by a Sirius red staining, did not differ between the two groups (Fig. 3E). Together these data imply that fibroblast-specific Endoglin deletion leads to expansion of the stromal compartment without affecting the balance between epithelial proliferation and apoptosis in CRC.

Enhanced myeloid infiltration in fibroblast-specific endoglin knock out adenomas

Since our model depends on DSS induced inflammation to enhance AOM induced carcinogenesis, we investigated the composition of immune infiltrates in the AOM/DSS-induced adenomas. At the end of the experiment, adenomas of three mice per group were analyzed by flow cytometry. Total immune infiltrates, based on the percentage of CD45 positive cells, was not significantly altered between the control and ENG$^{Fib-/-}$ group, although a lower percentage of CD45+ cells was observed in the ENG$^{Fib-/-}$ group (Fig.4A). Interestingly, when we determined the percentage of CD11b-expressing myeloid cells in the CD45+ population, increased infiltration was observed in ENG$^{Fib-/-}$ adenomas (Fig.4B). To further specify which cells of the myeloid population were increased, the abundance of macrophages was determined by assessing the percentage of F4-80 and Ly6C positive and negative cells . Although Ly6C+ monocytes

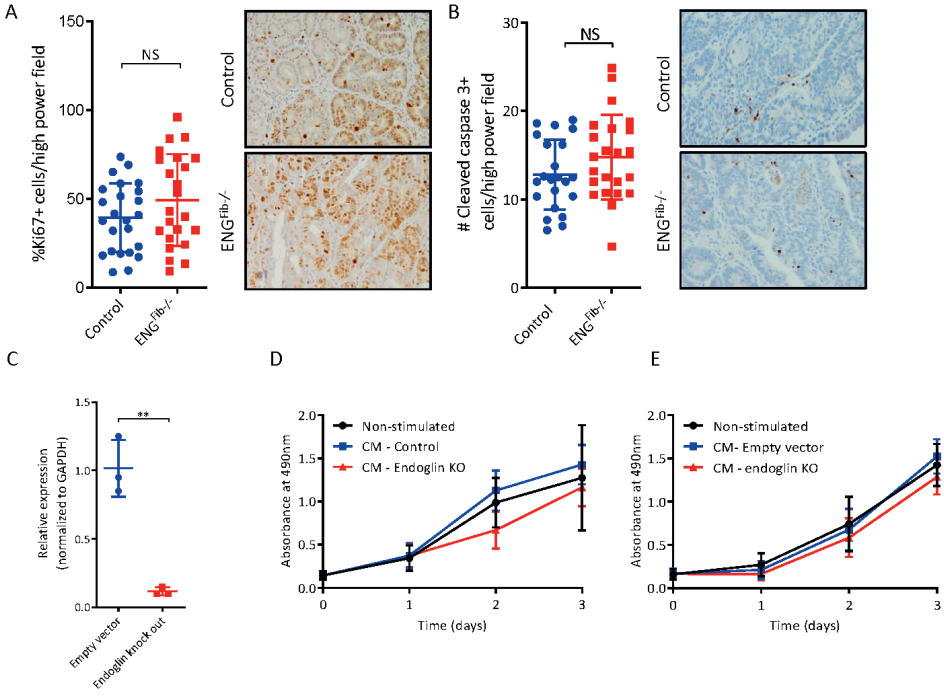

Figure 2. Proliferation in adenomas is not affected by endoglin deletion in fibroblasts. **A** Cellular proliferation in tumors was assessed by Ki67 staining and was similar in the control and ENGFibfl/fl group. **B** Cleaved caspase 3 was assessed to investigate the number of apoptotic cells which was similar in controls and ENGFibfl/fl group. n=24/23 tumors per group from two independent experiments. **C** MEFs were transduced with a Cre expressing lentivirus or empty vector control and endoglin expression was significantly reduced after transduction with Cre recombinase. Graph represents mean of three independent experiments. Stimulation with conditioned medium from MEFs, either empty vector or Cre recombinase transduced, did not affect tumor cell proliferation in CT26 (**D**) or MC38 cells (**E**). Graphs represent mean of three independent experiments performed in triplicate.

appeared to be increased in the ENG$^{Fib-/-}$ group, this did not reach statistical significance (Fig.4C). The percentage of Ly6C- macrophages, was significantly increased in ENG$^{Fib-/-}$ adenomas when compared with controls (Fig.4D). Indeed, increased macrophage recruitment to ENG$^{Fib-/-}$ adenomas was confirmed by quantifying immunohistochemical staining for the macrophage marker F4/80 (Fig.4E). Additionally, we assessed the percentage of neutrophils in adenomas using Ly6G stainings. Flow cytometry analysis showed that the percentage of Ly6G+ cells in the CD45+ population was strongly increased in the ENG$^{Fib-/-}$ group when compared with control mice, respectively 6% to 15% (Fig.4F). The number of Ly6G+ cells in adenomas was also assessed by IHC, and this analysis confirmed higher neutrophil infiltrate upon fibroblast-specific endoglin knock out (Fig. 4G). These data suggest that fibroblast-specific deletion of endoglin results in enhanced recruitment of myeloid cells, especially in neoplastic adenomas.

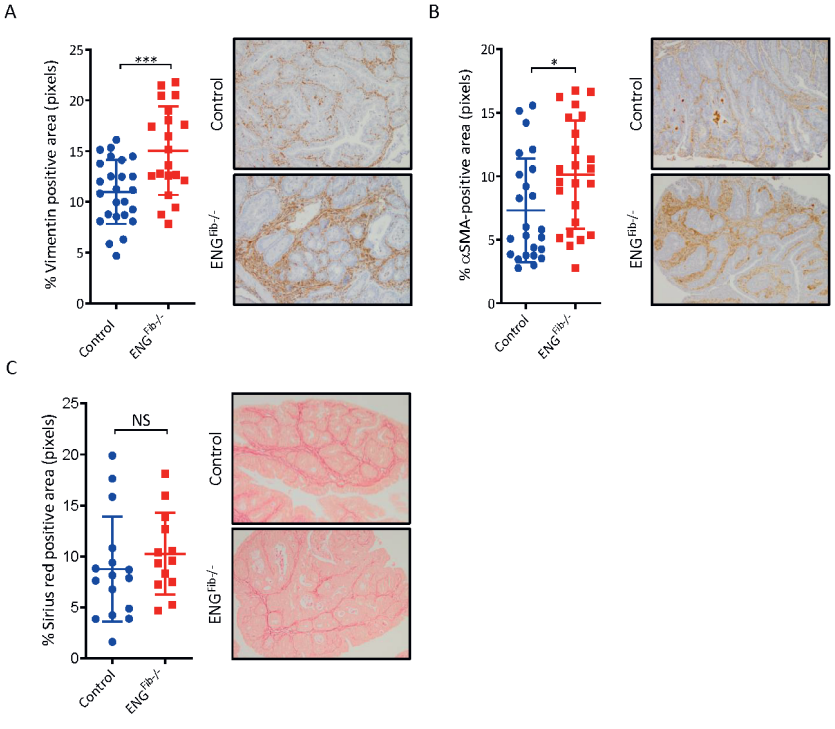

Figure 3. Endoglin deletion in fibroblasts increases stromal component in AOM/DSS-induced lesions. **A**. Lesions derived from control and ENGFibfl/fl mice were morphologically similar and were characterized as adenomas with high grade dysplasia. Total stroma content (**B**) and the abundance of activated fibroblasts (**C**) was assessed and proved to be increased after fibroblast-specific endoglin deletion. **D**. Total collagen deposition was not affected by endoglin knock out in fibroblasts. Data represent 29-25 mice/group from two independent experiments, average number of positive pixels. *P≤0.05, ***P≤0.001.

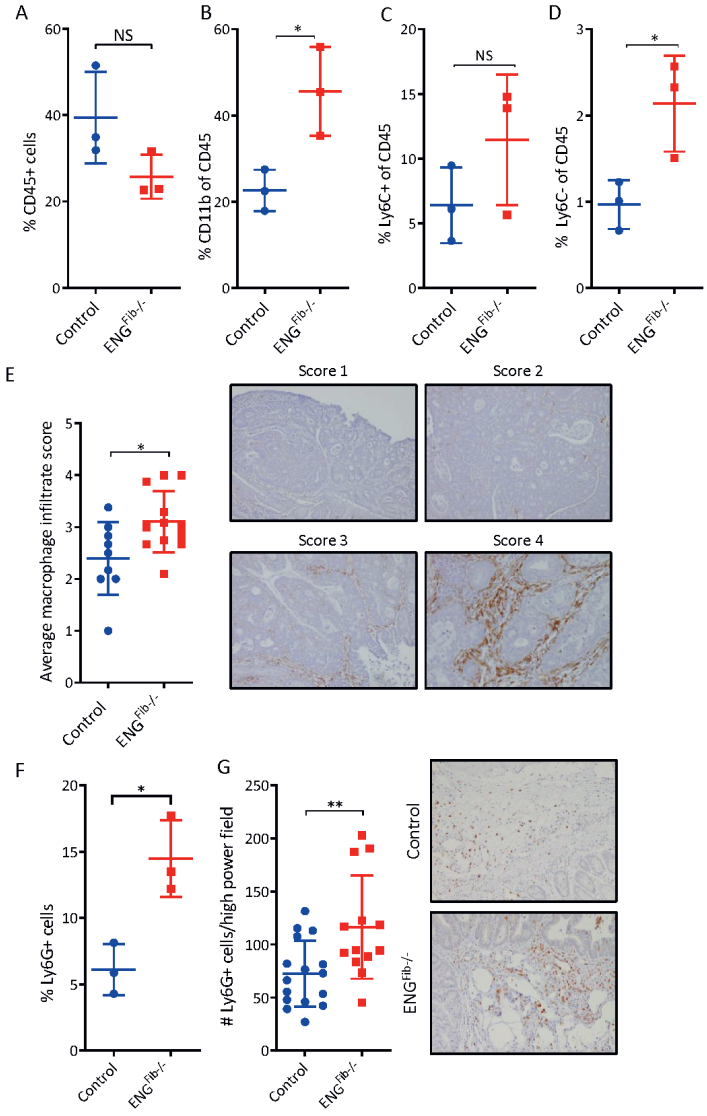

Figure 4. Increased macrophage recruitment to ENGFibfl/fl lesions. Immune cell infiltrate in the lesions was determined using flow cytometry. CD45+ cells were gated out of the life cell population (**A**). Subsequently, CD11b+ cells were gated out of CD45+ (**B**). Next, F4/80 expressing cells were selected from the CD11b+ population. Using Ly6C expression, subdivision between Ly6C+ monocytes (**C**) and Ly6C- macrophages (**D**) cells was made. (n=3 tumors/group) **E**. The extent of macrophage infiltration was scored based on F4/80 IHC. Score 1; ≤5% stroma positive, score 2; 5-25% stroma positive, score 3; 25-50% stroma positive, score 4; ≥50% stroma positive. (n= 11-12 tumors/group). *P≤0.05. Fibroblast-specific endoglin deletion increases neutrophil recruitment. **F**. Flow cytometry showed increased neutrophil infiltrate in ENGFibfl/fl lesions. Neutrophils were selected by gating for Ly6G in the CD45+/CD11b+ population. (n=3 tumors/group) **G**. IHC for Ly6G confirmed increased neutrophil influx in ENGFibfl/fl lesions. Graph represents 29/25 mice per group from two independent experiments, average number of Ly6G+ cells. *P≤0.05, **P≤0.01.

Neutrophils not responsible for the increased adenoma formation in the ENG$^{Fib-/-}$

Since the AOM DSS model is largely dependent on the presence of neutrophils and an increase in the number of neutrophils was observed in the adenomas, we investigated their role. First, we investigated the role of neutrophils during the formation of adenomas in the second DSS cycle, as indicated in [Fig. 5A]. Successful depletion of neutrophils was confirmed by flowcytometric analysis of the blood (Fig. 5B). The depletion was successful for three weeks and after that period, neutrophils started to re-appear, . At the end of the experiment mice were sacrificed, and intestinal adenomas were counted. As expected, a significant difference was seen between the ENG$^{Fib-/-}$ and the control samples. However, no differences were detected between the ENG$^{Fib-/-}$ and the ENG$^{Fib-/-}$ ly6G depleted group and the appropriate controls (Fig. 5C). Suggesting that neutrophils did not play a crucial role in the formation of the adenomas in this phase.

To investigate the possibility that neutrophils play a more crucial role in earlier stages of carcinogenesis in this model, they were depleted in the first DSS cycle in a follow-up experiment (Fig. 5D). Neutrophil depletion remained effective for 3 weeks (Fig. 5E). When mice were sacrificed after 13 weeks, a decrease in the number of adenomas within the ly6G depleted group [Fig. 5F]. However, once we calculated the relative number of adenomas, there was no difference between the controls and the ly6G depleted samples [Fig. 5G]. These data suggest that Ly6G+ neutrophils are important for the formation of adenomas in the AOM DSS model but do not seem to contribute to the increased lesion formation in the ENG$^{Fib-/-}$mice.

Loss of myeloid and Ly6C positive immune cells in blood and intestine from the ENG$^{Fib-/-}$ mice

Since ENG$^{Fib-/-}$ mice lost significantly more weight especially during the first DSS cycle we hypothesized that this could be due to increased inflammation, thereby enhancing lesion formation. To test this hypothesis, we performed a short-term DSS experiment to assess inflammation in the ENG$^{Fib-/-}$ *mice* versus control mice. During DSS treatment mice from the ENG$^{Fib-/-}$ lost significantly more weight than the controls (Fig. 6A). When the mice were sacrificed, a macroscopic disease score was performed [27, 28] to analyze the severity of the intestines' inflammation, stool, and general colonic conditions, which revealed a significant increase in the macroscopic disease score suggesting more tissue damage and inflammation (Fig. 6B). However, this was not reflected in the relative weight of the intestine which was significantly decreased in the ENG$^{Fib-/-}$ *mice* (Fig. 6C).

To further explore the composition of the intestinal immune infiltrate, colons were processed for flow cytometry. The number of CD45+ cells within the colon showed no differences, as shown in figure 6D, suggesting that the inflammation might not be different within the colon. However, the composition of the immune cells was changed. Interestingly, as observed in the blood, a decrease in CD11B+ myeloid cells

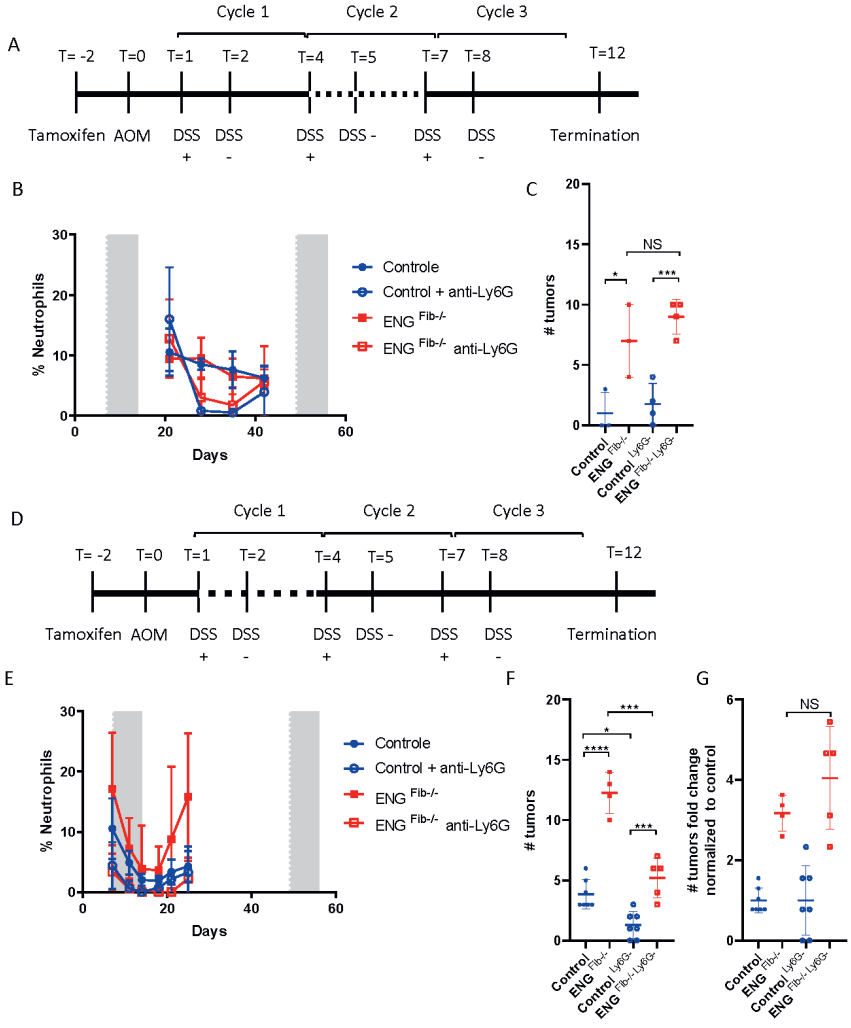

Figure 5. Neutrophils not responsible for the increased adenoma formation in the ENGFib-/-.
A experimental setup of the results presented in **B** and **C**. **B** decrease un the % of neutrophils up on depletion with a neutrophil depleting antibody. C Number of lesions which showed no difference between the neutrophil depleted group ENGFib-/- and ENGFib+/+. **D** experimental setup for the results presented in **E** and **F**. **E** decrease un the % of neutrophils up on depletion with a neutrophil depleting antibody. **F** number of lesions showing no difference between the neutrophil depleted groups ENGFib-/- and ENGFib+/+ data normalized to control (**G**).

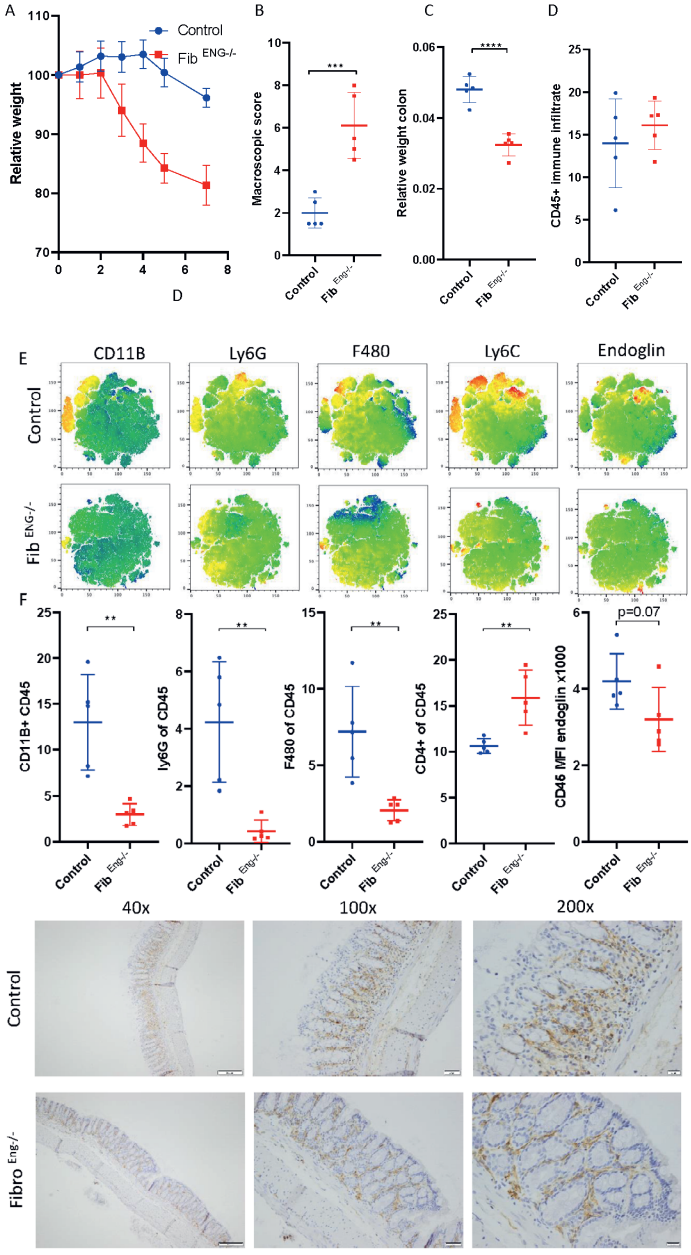

Figure 6. ***Loss of myeloid and Ly6C positive immune cells in blood and intestine from the ENGFib-/- mice.*** **A** short-term DSS experiment to assess inflammation in the ENGFib-/- *mice* versus control mice. ENGFib-/- lost significantly more weight than the controls (**A**). increase in the macroscopic disease score (**B**) no difference in relative weight of the intestine (**C**) the ENGFib-/- *mice*. (**D**) no difference in the total number of infiltrating immune cells (CD45+). Flow-cytometic analysis revealed a loss of myeloid and ly6C positive immune cells in the intestine from the ENGFib-/- mice presented as a TSME plot (RED high expression Bleu low expression) in **F** these results were plotted and showed decreased myeloid cells. Endoglin expression was assessed on CD45+ cells which showed to be decreased in the ENGFib-/- mice.

were observed in the intestines (Fig 6E and quantified in Fig. 6F). This is the same immune profile as seen in the blood of the ENG$^{Fib-/-}$ mice. Interestingly, a decrease endoglin (p=0.07) mean fluorescent intensity on CD45+ cells was observed in the ENG$^{Fib-/-}$ mice. This might indicate a decrease in endoglin expressing CD45+ cells or reduced recruitment of endoglin expressing CD45 cells.
Similar findings were observed in collagen1α2-CreERT2.ENG*fl/fl* mice (supplementary figure 2 and 3). These results might indicate hampered recruitment or proliferation/ differentiation of monocytes in both blood and intestine but this needs to be further evaluated.

DISCUSSION

This study shows that fibroblast-specific endoglin deletion increases tumorigenesis in a mouse model for colitis-associated CRC. Fibroblast specific endoglin deletion did not affect epithelial cell proliferation in adenomas but resulted in stromal expansion and increased influx of macrophages and neutrophils into the adenomas. However, this influx of neutrophils was not responsible for the increased tumorigenesis as shown by a ly6G depletion. Although increased numbers of myeloid cells were observed in late stages of intestinal lesion formation in the ENG$^{Fib-/-}$ mice, the opposite was observed in both the intestines as well as the blood in DSS induced colitis. Therefore, the underlining cause of the increased tumorigenesis is still unclear.
The immune system plays an important role during tumor development and progression. Neutrophils (ly6G positive) have been reported to be essential for the formation of tumors in the AOM DSS model [29, 30]. We show indeed that these cells play an important role in the AOM DSS tumor model. However, the increased tumorigenesis caused by the fibroblast specific endoglin deletion did not seem to be provoked by the influx of Ly6G positive cells, since depletion of the neutrophils did not abrogate the increased lesion formation.
Previously it was shown that adoptive transfer of ly6C high monocytes limits bacterial translocation and intestinal damage [31]. We found a decreased ly6C high profile during a short DSS experiment both in the blood of the ENG$^{Fib-/-}$ mice as in the intestines of the ENG$^{Fib-/-}$ mice, suggesting that loss of these cells increases intestinal adenoma formation by increased bacterial translocation, which might partially be reflected in the increased intestinal macroscopic score. Changes in immune composition were observed and the hampered intestinal ly6C high influx might be explained by altering the cytokine expression by the fibroblast specific endoglin knockout in the intestines or the bone marrow. However, this has not been examined and needs to be further explored.

During inflammation pro-inflammatory cytokines such as IFNγ, IL1β and TNFα activate progenitors in the bone marrow to differentiate into myeloid effector cells. These progenitor cells or hematopoietic stem/progenitor cells (HSPC) express both Col1a1 and Col1a2 [32], which might suggest that we have also performed an endoglin knockout on HSPCs. Interestingly, we found no evidence of endoglin knockout on myeloid cells since there was no difference in endoglin expression on CD45+ CD11B+ cells when compared to the controls. However, CD45+ Ly6C+ CD11B- cells have been reported to be monocyte-macrophage progenitors cells which showed a reduction (p=0.051) of endoglin in the blood of mice up on fibroblast (Col1a1 and Col1a2) specific endoglin deletion. Mice lacking endoglin in macrophages show an impaired phagocytic activity. The altered immune activity of endoglin deficient subsets might explain the higher rate of infectious disease seen in HHT1 patients [33] and partially the phenotypic differences in the $ENG^{Fib-/-}$ mice.

The interplay between stroma and epithelium is crucial during intestinal homeostasis. Imbalance in this paracrine interaction can lead to decreased epithelial apoptosis or an increase in stem-cell proliferation [34], both resulting in spontaneous polyp formation. Inactivation of the BMP pathway by knocking out the BMP receptor type II (BMPRII) in intestinal stromal cells [35], increased epithelial cell proliferation and resulted in local polyp formation in mouse intestine [35]. Similar effects were observed for the TGF-β receptor type II (TGF-βRII) deletion in fibroblasts [36]. Inactivation of BMPRII or TGF-βRII leads to tumor formation within seven weeks in the colorectum or stomach, respectively [35, 36]. Our study did not observe spontaneous tumor formation after endoglin deletion in fibroblasts during the 13-week experimental period. Our *in vitro* proliferation data supported this observation, where stimulation with conditioned medium from endoglin knock out MEFs did not affect proliferation in two mouse CRC cell lines. Although no spontaneous tumors developed, fibroblast-specific endoglin deletion enhanced chemically-induced adenoma formation. One of the differences between adenomas from the control and $ENG^{Fib-/-}$ group, was the increase of activated fibroblasts upon endoglin knock out. In CRC patients, the abundance of tumor stroma has been reported to be prognostic for both overall and metastasis-free survival [37]. This could imply that $ENG^{Fib-/-}$ adenomas would be more aggressive and could have a higher malignant potential. However, the severity of animal discomfort in our model does not allow for a prolonged experimental period, therefore tumor progression and metastatic spread could not be evaluated.

Our data regarding the SMA content of the adenomas are not in accordance with pharmacological and genetic data showing that treatment with the endoglin neutralizing antibody TRC105 reduced αSMA-positive tumor content in an *in vivo* breast cancer model [38]. Additionally, endoglin heterozygous mice displayed reduced αSMA-positive content in prostate cancer [39]. A major difference between

the studies mentioned earlier and our current research is that heterozygote endoglin deletion and TRC015 treatment affect all cells expressing endoglin, which might explain the differential effects observed compared to fibroblast-specific endoglin deletion.

In summary, these data show that fibroblast specific loss of endoglin increases intestinal adenoma formation in a model for colitis associated cancer. These lesions show increased stromal accumulation and altered immune cell infiltration, which might be involved in the increased carcinogenesis. Further studies should reveal the exact role of the altered immune cell infiltration.

Acknowledgements

This study was supported by the Alpe d'HuZes/ Bas Mulder award 2011 (UL2011-5051) to LH. We thank Kirsten Lodder (Dept. Molecular Cell Biology, LUMC) and Marij Mieremet (Dept. Gastroenterology-Hepatology, LUMC) for technical support.

REFERENCES

1. Herrera, M., et al., *Functional heterogeneity of cancer-associated fibroblasts from human colon tumors shows specific prognostic gene expression signature.* Clin Cancer Res, 2013. **19**(21): p. 5914-26.

2. Hawinkels, L.J., et al., *Interaction with colon cancer cells hyperactivates TGF-beta signaling in cancer-associated fibroblasts.* Oncogene, 2014. **33**(1): p. 97-107.

3. Nyberg, P., T. Salo, and R. Kalluri, *Tumor microenvironment and angiogenesis.* Front Biosci, 2008. **13**: p. 6537-53.

4. Henriksson, M.L., et al., *Colorectal cancer cells activate adjacent fibroblasts resulting in FGF1/FGFR3 signaling and increased invasion.* Am J Pathol, 2011. **178**(3): p. 1387-94.

5. Sahai, E., et al., *A framework for advancing our understanding of cancer-associated fibroblasts.* Nat Rev Cancer, 2020. **20**(3): p. 174-186.

6. Tommelein, J., et al., *Cancer-associated fibroblasts connect metastasis-promoting communication in colorectal cancer.* Front Oncol, 2015. **5**: p. 63.

7. Ronnov-Jessen, L., et al., *The origin of the myofibroblasts in breast cancer. Recapitulation of tumor environment in culture unravels diversity and implicates converted fibroblasts and recruited smooth muscle cells.* J Clin Invest, 1995. **95**(2): p. 859-73.

8. Lewis, M.P., et al., *Tumour-derived TGF-beta1 modulates myofibroblast differentiation and promotes HGF/SF-dependent invasion of squamous carcinoma cells.* Br J Cancer, 2004. **90**(4): p. 822-32.

9. Li, D.Y., et al., *Defective angiogenesis in mice lacking endoglin.* Science, 1999. **284**(5419): p. 1534-7.

10. Carvalho, R.L., et al., *Defective paracrine signalling by TGFbeta in yolk sac vasculature of endoglin mutant mice: a paradigm for hereditary haemorrhagic telangiectasia.* Development, 2004. **131**(24): p. 6237-47.

11. Arthur, H.M., et al., *Endoglin, an ancillary TGFbeta receptor, is required for extraembryonic angiogenesis and plays a key role in heart development.* Dev Biol, 2000. **217**(1): p. 42-53.

12. Lebrin, F., et al., *Endoglin promotes endothelial cell proliferation and TGF-beta/ALK1 signal transduction.* EMBO J, 2004. **23**(20): p. 4018-28.

13. Nolan-Stevaux, O., et al., *Endoglin requirement for BMP9 signaling in endothelial cells reveals new mechanism of action for selective anti-endoglin antibodies.* PLoS One, 2012. **7**(12): p. e50920.

14. Tian, H., et al., *Endoglin mediates fibronectin/alpha5beta1 integrin and TGF-beta pathway crosstalk in endothelial cells.* EMBO J, 2012. **31**(19): p. 3885-900.

15. Goumans, M.J., et al., *Activin receptor-like kinase (ALK)1 is an antagonistic mediator of lateral TGFbeta/ALK5 signaling.* Mol Cell, 2003. **12**(4): p. 817-28.

16. Goumans, M.J., et al., *Balancing the activation state of the endothelium via two distinct TGF-beta type I receptors.* EMBO J, 2002. **21**(7): p. 1743-53.

17. ten Dijke, P., M.J. Goumans, and E. Pardali, *Endoglin in angiogenesis and vascular diseases.* Angiogenesis, 2008. **11**(1): p. 79-89.

18. Romero, D., et al., *Endoglin regulates cancer-stromal cell interactions in prostate tumors.* Cancer Res, 2011. **71**(10): p. 3482-93.

19. Paauwe, M., et al., *Endoglin Expression on Cancer-Associated Fibroblasts Regulates Invasion and Stimulates Colorectal Cancer Metastasis.* Clin Cancer Res, 2018. **24**(24): p. 6331-6344.

20. Tanaka, T., et al., *A novel inflammation-related mouse colon carcinogenesis model induced by azoxymethane and dextran sodium sulfate.* Cancer Sci, 2003. **94**(11): p. 965-73.

21. Neufert, C., C. Becker, and M.F. Neurath, *An inducible mouse model of colon carcinogenesis for the analysis of sporadic and inflammation-driven tumor progression.* Nat Protoc, 2007. **2**(8): p. 1998-2004.

22. Corbett, T.H., et al., *Tumor induction relationships in development of transplantable cancers of the colon in mice for chemotherapy assays, with a note on carcinogen structure.* Cancer Res, 1975. **35**(9): p. 2434-9.

23. Brattain, M.G., et al., *Establishment of mouse colonic carcinoma cell lines with different metastatic properties.* Cancer Res, 1980. **40**(7): p. 2142-6.

24. Larsson, J., et al., *Abnormal angiogenesis but intact hematopoietic potential in TGF-beta type I receptor-deficient mice.* EMBO J, 2001. **20**(7): p. 1663-73.

25. Allinson, K.R., et al., *Generation of a floxed allele of the mouse Endoglin gene.* Genesis, 2007. **45**(6): p. 391-5.

26. Hawinkels, L.J., et al., *Tissue level, activation and cellular localisation of TGF-beta1 and association with survival in gastric cancer patients.* Br. J. Cancer, 2007. **97**(3): p. 398-404.

27. Cooper, H.S., et al., *Clinicopathologic study of dextran sulfate sodium experimental murine colitis.* Lab Invest, 1993. **69**(2): p. 238-49.

28. Molendijk, I., et al., *Intraluminal Injection of Mesenchymal Stromal Cells in Spheroids Attenuates Experimental Colitis.* J Crohns Colitis, 2016. **10**(8): p. 953-64.

29. Shang, K., et al., *Crucial involvement of tumor-associated neutrophils in the regulation of chronic colitis-associated carcinogenesis in mice.* PLoS One, 2012. **7**(12): p. e51848.

30. Jamieson, T., et al., *Inhibition of CXCR2 profoundly suppresses inflammation-driven and spontaneous tumorigenesis.* J Clin Invest, 2012. **122**(9): p. 3127-44.

31. Seregin, S.S., et al., *NLRP6 function in inflammatory monocytes reduces susceptibility to chemically induced intestinal injury.* Mucosal Immunol, 2017. **10**(2): p. 434-445.

32. Charbord, P., et al., *A systems biology approach for defining the molecular framework of the hematopoietic stem cell niche.* Cell Stem Cell, 2014. **15**(3): p. 376-391.

33. Cirulli, A., et al., *Patients with Hereditary Hemorrhagic Telangectasia (HHT) exhibit a deficit of polymorphonuclear cell and monocyte oxidative burst and phagocytosis: a possible correlation with altered adaptive immune responsiveness in HHT.* Curr Pharm Des, 2006. **12**(10): p. 1209-15.

34. Hu, J.L., et al., *CAFs secreted exosomes promote metastasis and chemotherapy resistance by enhancing cell stemness and epithelial-mesenchymal transition in colorectal cancer.* Mol Cancer, 2019. **18**(1): p. 91.

35. Beppu, H., et al., *Stromal inactivation of BMPRII leads to colorectal epithelial overgrowth and polyp formation.* Oncogene, 2008. **27**(8): p. 1063-70.

36. Bhowmick, N.A., et al., *TGF-beta signaling in fibroblasts modulates the oncogenic potential of adjacent epithelia.* Science, 2004. **303**(5659): p. 848-51.

37. Mesker, W.E., et al., *The carcinoma-stromal ratio of colon carcinoma is an independent factor for survival compared to lymph node status and tumor stage.* Cell Oncol, 2007. **29**(5): p. 387-398.

38. Paauwe, M., et al., *Endoglin targeting inhibits tumor angiogenesis and metastatic spread in breast cancer.* Oncogene, 2016.

39. Romero, D., et al., *Endoglin regulates cancer-stromal cell interactions in prostate tumors.* Cancer Res, 2011. **71**(10): p. 3482-3493.

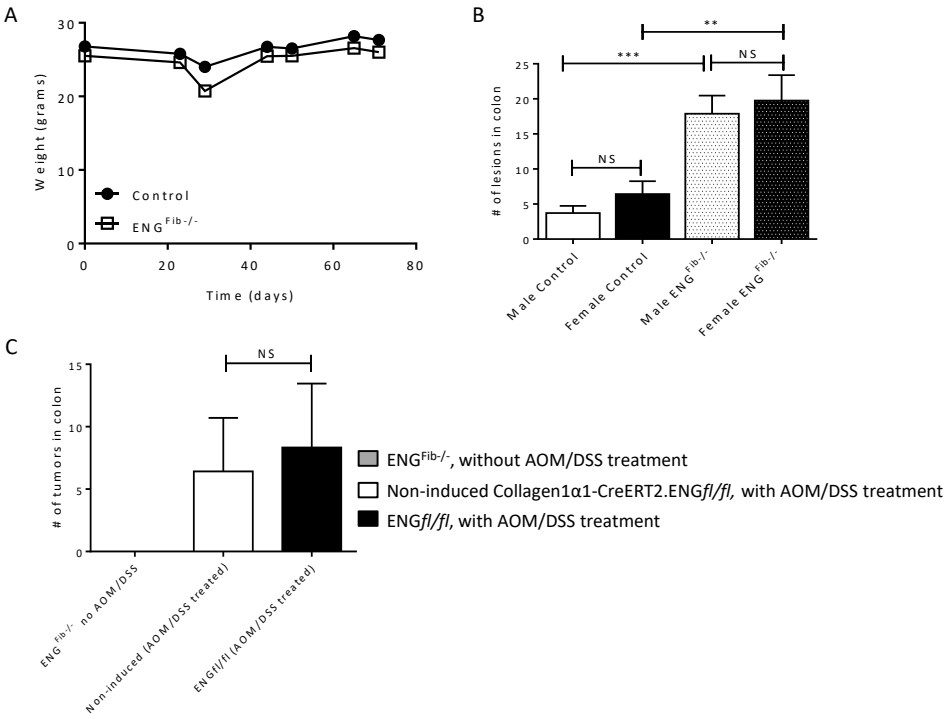

Supplementary figure 1 A. Mouse weights dropped during DSS supplementation, but recovered during the two weeks on normal drinking water. **B.** The number of lesions observed in the AOM/DSS model is independent of animal sex, in both the control and ENGFib-/- group. **C.** Fibroblast-specific endoglin deletion without AOM/DSS treatment did not induce neoplastic growth over the course of 13 weeks (n=8). ENGfl/fl mice, which received tamoxifen, showed similar number of lesions as non-induced Collagen1α1-CreERT2. ENGfl/fl mice after AOM/DSS (n=9).

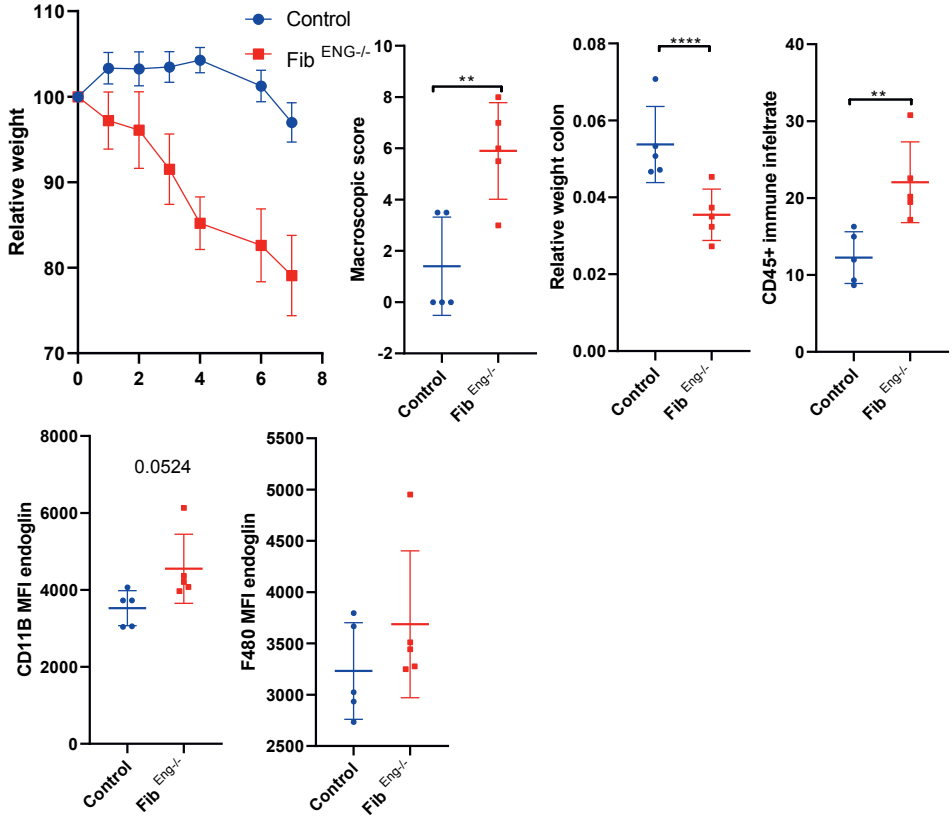

Supplementary figure 2. collagen1α2-CreERT2.ENGfl/fl mice

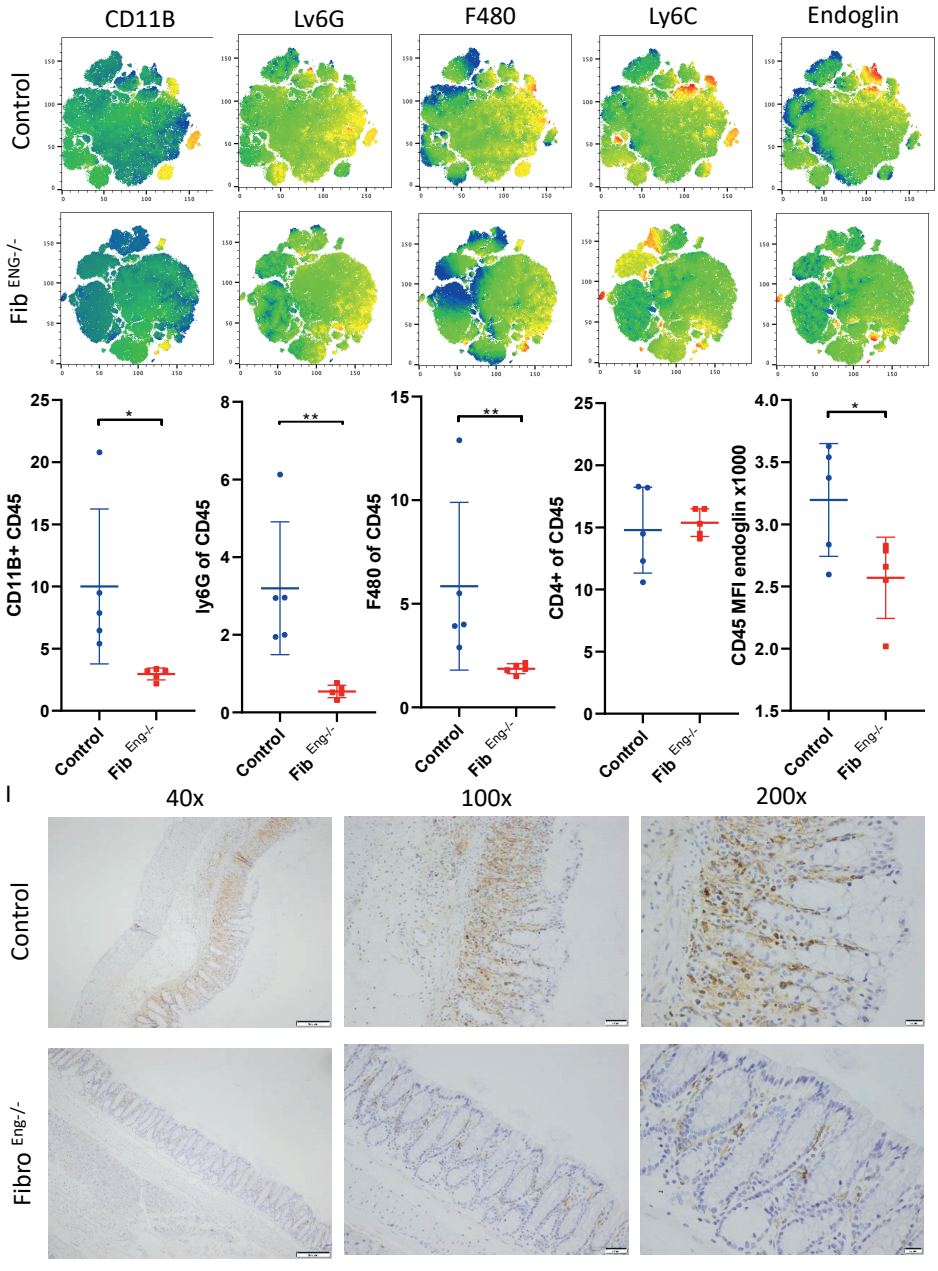

Supplementary figure 3. collagen1α2-CreERT2.ENGfl/fl mice